Anal Bioanal Chem (2009) 394:421–425
DOI 10.1007/s00216-008-2550-6

ORIGINAL PAPER

Detecting proteins complex formation using steady-state diffusion in a nanochannel

Nicolas F. Y. Durand · Elli Saveriades · Philippe Renaud

Received: 29 September 2008 / Revised: 24 November 2008 / Accepted: 27 November 2008 / Published online: 14 December 2008

Abstract In this work, we present theoretical and experimental studies of nanofluidic channels as a potential biosensor for measuring rapid protein complex formation. Using the specific properties offered by nanofluidics, such as the decrease of effective diffusion of biomolecules in confined spaces, we are able to monitor the binding affinity of two proteins. We propose a theoretical model describing the concentration profile of proteins in a nanoslit and show that a complex composed by two bound biomolecules induces a wider diffusion profile than a single protein when driven through a nanochannel. To validate this model experimentally, we measured the increase of the fluorescent diffusion profile when specific biotinylated dextran was added to fluorescent streptavidin. We report here a direct and relatively simple technique to measure the affinity between proteins.

Keywords Bioassay · Nanofluidics · Nanochannel · Fluorescence · Proteomics · Microfabrication

Introduction

Nanofluidics is becoming a major field of research [1] and has been applied in microfluidic systems allowing for DNA manipulation [2], protein separation [3], sample preconcentration [4], and single molecule detection [5]. One of the characteristic physical effects of nanofluidics is the interaction of biomolecules with the channel surfaces, which greatly reduces their effective diffusion coefficient. Williams et al. [6] have demonstrated the possibility to detect solute concentration by measuring diffusion change in a microfluidic T-sensor and Hatch et al. [7] have reused this principle to detect immunobinding.

In this work, we exploit this property and present a protein-binding affinity bioassay based on steady-state diffusion in a nanochannel.

Our device, shown in Fig. 1, consists of a narrow nanochannel of width w and length L_{nC}. This runs into short nanoslit of length L_{nS} with the same nanometer dimension height h_{nS} as the main nanochannel. The nanoslit then spills into a deep microchannel of height $h_{\mu C} \gg h_{nS}$. Fluorescently labeled molecules at the inlet of the nanochannel are drawn into the nanochannel by applying a constant negative pressure at the microchannel outlet. As recently reported by Durand et al. [8], when biomolecules enter a nanoslit from an adjacent nanochannel, they disperse laterally. The lateral dispersion is affected by diffusion of molecules: decreasing diffusion extends lateral dispersion because molecules stay longer along their flow line before diffusing into the main microchannel. This phenomenon is used in the present study to measure proteins complex formation.

Theory

In our model, we assume that solutions are dilute and incompressible, there are no chemical reactions except between proteins, and that external forces and mass transport are only due to diffusion and convection. We assume that local electrical phenomena due to streaming potential are negligible. We assume that we draw biomolecules into the nanochannel from a large reservoir, keeping the concentration c_0 in the nanochannel constant. As the nanochannel height is 200 times lower than its width, we

N. F. Y. Durand (✉) · E. Saveriades · P. Renaud
Microsystems Laboratory, STI-LMIS, EPFL,
1015 Lausanne, Switzerland
e-mail: nicolas.durand@epfl.ch

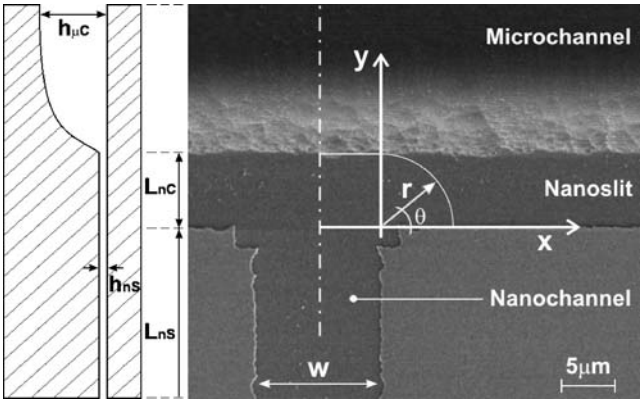

Fig. 1 Top view SEM picture of a nanochannel and a nanoslit, defined by the thickness of the amorphous silicon (h_{nS}=50 nm, $h_{\mu C}$= 5 μm, w=10 μm, L_{nS}=7 μm, L_{nC}=20 μm). The *left scheme* represents cross sections of the nanochannel, the nanoslit, and the microchannel (not to scale)

obtain a flat velocity profile for the injected florescent plug in the x–y plan. We assume that the effective diffusion coefficients of molecules in the nanochannel are much smaller than in normal bulk diffusion due to their interaction with the nanochannel surfaces [8]. Consequently, mass transport is primarily convective rather than diffusive. When the plug front enters the nanoslit located at the end of the nanochannel, it expands in a "flat half-circle" shape before flowing into the microchannel as illustrated in Figs. 2 and 4.

This simplified description of the front profile of the biomolecules is valid for an infinitely long nanoslit and is an acceptable approximation in our case. By simplifying the validity of the equation of continuity [9], from the nanochannel-slit transition, we observe a decrease of the average flow velocity u_r along the semi-circular flow front

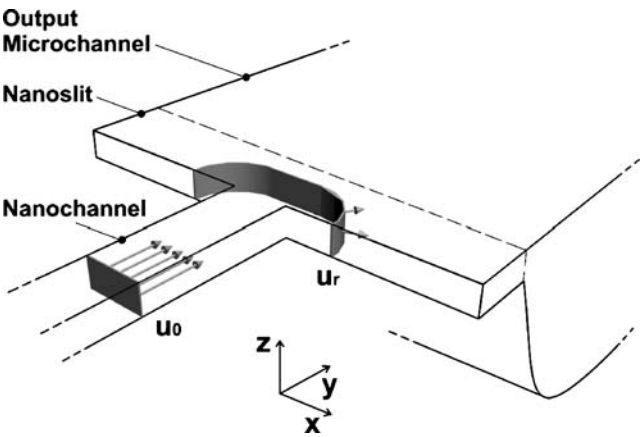

Fig. 2 3D schematic of the nanofluidic system (not to scale). Flow directions in the nanochannel and in the nanoslit are illustrated by *3D arrows*. In the nanochannel, the flow velocity u_0 remains constant, whereas the flow front is expanding in the nanoslit, leading to a decrease of the average flow velocity $u_r(x,y)$

at the $r=(x^2+y^2)^{0.5}$ position as the biomolecule plug front moves away from the nanochannel:

$$u_r(r) \cong u_0 \frac{w}{\pi r + w} \tag{1}$$

where u_0 is the initial flow velocity in the nanochannel and w the nanochannel width.

Integrating Eq. 1 with respect to r gives:

$$t(r) = \frac{\pi r^2}{2u_0 w} + \frac{r}{u_0} \tag{2}$$

Next, we assume that the liquid passing through the channel-slit transition from the nanochannel has a fixed concentration c_0. The output microchannel serves as a sink, where the concentration of proteins is maintained closed to zero by slow microchannel flow of pure buffer solution. The concentration profile of the proteins along the nanochannel and the nanoslit is derived for the three principle cases: (1) diffusion is the only transport mechanism for proteins, i.e., no flow velocity through the nanochannel is applied, a steady-state diffusion profile is obtained, which is independent of the diffusion coefficient. (2) The diffusion coefficient is null or the velocity in the nanochannel u_0 is infinite, then a constant concentration c_0 along the nanochannel and the nanoslit is obtained. (3) The intermediate case for finite diffusion coefficient: adapting the model of unsteady diffusion in a semi infinite slab described by Cussler [10], we find that the concentration profile $c(r)$ in the nanoslit in this last case is:

$$c(r) = c_0 \times \mathrm{erf}\left(\frac{R_{nS} - r}{\sqrt{4Dt}}\right) \tag{3}$$

where $R_{nS}=L_{nS}/\sin\theta$ is the distance inside the nanoslit between the channel-slit transition and the microchannel. c_0 is the biomolecule concentration in the nanochannel. D is the diffusion coefficient; erf the error function defined by:

$$\mathrm{erf}\varsigma = \frac{2}{\sqrt{\pi}} \int_0^{\varsigma} \mathrm{e}^{-s^2} ds \tag{4}$$

This model is only valid if the nanochannel and nanoslit lengths L_{nC} and L_{nS} are large enough that the biomolecule concentration is close to c_0 when entering the nanochannel. Assuming an infinite source of biomolecules at concentration c_o, the diffusion profile achieves a steady state and Eqs. 2 and 3 can be combined:

$$c(r) = c_0 \times \mathrm{erf}\left(\frac{R_{nS} - r}{\sqrt{\frac{D}{u_0} \times \left(\frac{2\pi(R_{nS}-r)^2}{w} + 4(R_{nS} - r)\right)}}\right) \tag{5}$$

Figure 3 illustrates the concentration profile as a function of the distance in the nanoslit from the nanochannel-slit transition as described by Eq. 5, for different values of the

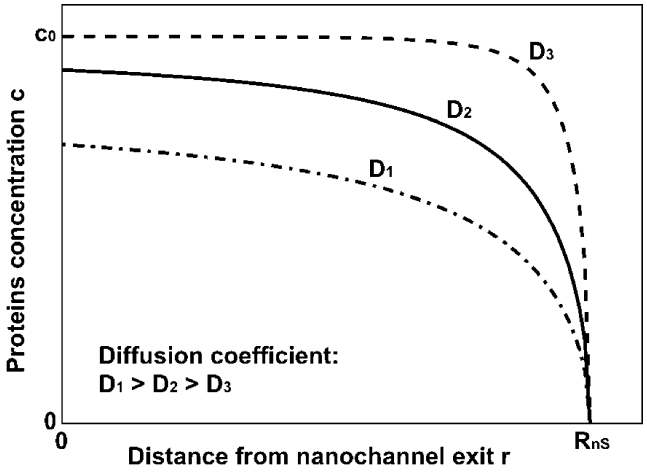

Fig. 3 Steady diffusion of proteins through a 2D nanoslit from the nanochannel exit (r=0) into the exit microchannel (r=R_{nS}) when a constant fluid velocity u_0 is applied. The curves are plotted using Eq. 5 and show that higher diffusion coefficients decrease the concentration profile

diffusion coefficient. For a given nanochannel velocity u_0, large molecules with a low diffusion coefficients take longer to pass through the nanochannel than small ones with higher diffusion coefficients, resulting in a larger dispersion distance in the lateral nanoslit. This effect is used to locally measure the diffusion coefficients, thus, formation of proteins complexes.

Experimental

Cleanroom microfabrication processes were used to produce the devices. Five-micrometer-deep microchannels were wet-etched on a Pyrex wafer and a 50-nm layer of amorphous silicon (aSi), which is used to define the height of the nanoslit, was sputtered and structured by plasma etching. A second Pyrex wafer, in which access holes were drilled by sandblasting, was anodically bonded onto the first wafer. Afterwards, the wafers were diced into individual chips. Figure 2 shows a SEM picture of a manufactured nanochannel.

The motion of fluorescently labeled proteins through the nanoslit was recorded by a single photon counting camera [LUCA EMCCD from Andor] connected to an inverted microscope [Axiovert S100 from Zeiss]. We assume that fluorescence intensity is proportional to the proteins concentration $c(r)$. We chose to neglect the effects of any disparities in the optical system (lenses aberration, filters quality, and lamp intensity fluctuations).

In our experiments, we used fluorescent streptavidin proteins, 53 kDa of molecular weight [streptavidin with Alexa Fluor® 633 from Molecular Probes], biotin–dextran, 10 kDa of molecular weight [from Sigma-Aldrich], and wheat germ agglutinin, 38 kDa of molecular weight [with Alexa Fluor® 633 from Molecular Probes]. We used PBS solution of pH 7.1 [phosphate-buffered saline from Sigma-Aldrich] containing 137 mM sodium chloride, 10 nM phosphate buffer, and 2.7 mM potassium chloride diluted with deionized water (18 MΩ cm). All solutions were prepared and degassed just before use. Solutions containing proteins were loaded into the microchannel inlet reservoir by syringe. The PBS solution was drawn through the microfluidic channel by air aspiration using an air-pressure regulator [from Bellofram Corp.] from 0 to −800 mbar.

Results and discussion

Figure 4 shows fluorescent biomolecules diffusing in the nanoslit area as observed through a standard fluorescence microscope. First, we injected 53 kDa fluorescently labeled streptavidin proteins and waited until we obtained the steady-state diffusion profile observed in Fig. 4a. We then injected 10 kDa biotinylated dextran in order to effect a substantial increase in complex weight for each binding event. Figure 4b represents the steady-state diffusion profile of the streptavidin–biotin–dextran complex after adding biotinylated dextran: the increase of fluorescence steady-state diffusion is clearly observed. We did the same

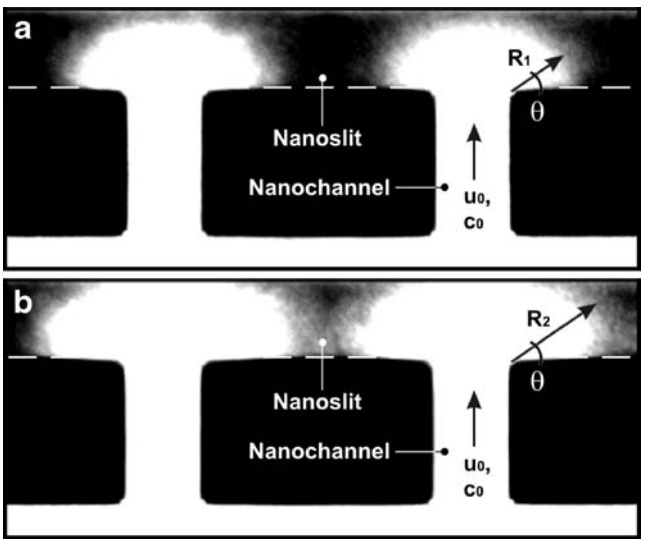

Fig. 4 Video images showing the steady-state diffusion of fluorescent species through the nanoslits (w=10 μm, L_{nS}=10 μm, L_{nC}=20 μm). **a** We injected c_0=2 μM fluorescent streptavidin proteins in the nanochannels by applying a pressure difference ΔP=0.3 bar (corresponding to u_0=120 nm/s) and measured the distance R_1 from the exit of the nanochannel to half fluorescence intensity $c_0/2$ for θ=45° angle. **b** We added 6 μM non-fluorescent biotinylated dextran and measured the increased length R_2 (at same ΔP and θ). The experiments are realized in PBS solution with pH of 7.1

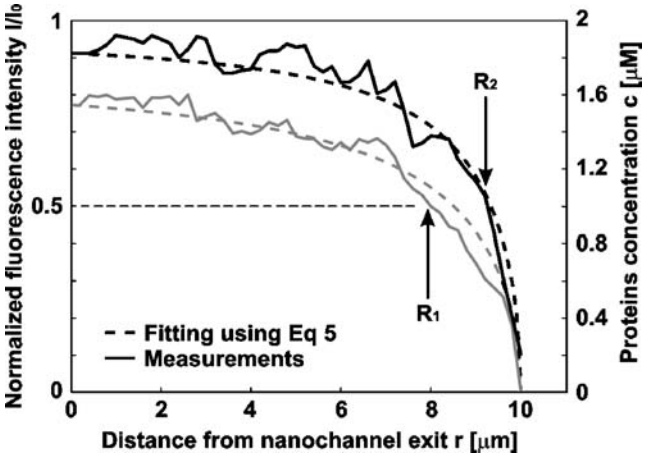

Fig. 5 Evolution of the concentration profile of proteins with the distance from nanochannel exit. The measurements were performed on video images with θ=90°, in same conditions as Fig. 4. *Gray lines* represent fluorescent streptavidin proteins (higher D) diffusion profile and *black ones* fluorescent streptavidin with biotin–dextran complex (lower D). *Lines* represent measurements and *dotted lines* are best fits using Eq. 5 with u_0=120 nm/s, L_{nS}=10 μm, L_{nC}=20 μm, D_1=1.6×10^{-13} m^2/s and D_2=8×10^{-14} m^2/s

experiment with 38 kDa wheat germ agglutinin as non-specific control, instead of biotin–dextran. As expected, there was no significant change in the diffusion profile.

We plot, in Fig. 5, the recorded fluorescence intensity in the nanoslit along r before and after adding the biotin–dextran solution. From the best fits using Eq. 5, we calculated the effective diffusion coefficients D_1=1.6×10^{-13} m^2/s and D_2=8×10^{-14} m^2/s for streptavidin and the streptavidin–biotin–dextran complex, respectively, The experiment was repeated several times with different flow velocities in the nanochannel.

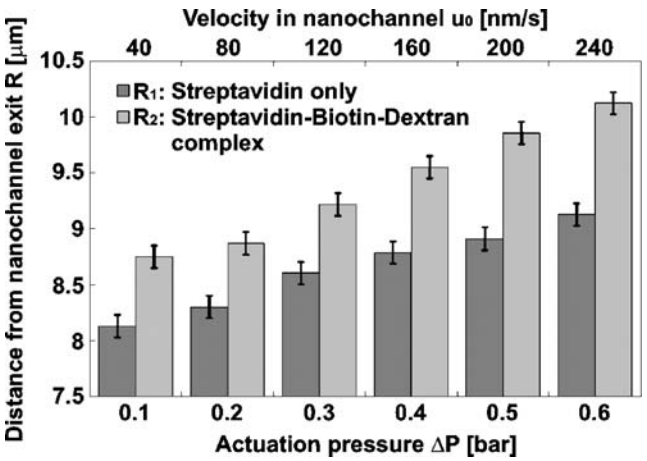

Fig. 6 Measured distances from nanochannel exit to half fluorescence intensity before (in *dark gray*) and after (in *light gray*) adding biotinylated dextran to fluorescent streptavidin diffusing in a nanoslit for different actuation pressure. The *error bars* indicate the error of reading when injecting the proteins. Conditions: θ=45°, w=10 μm, L_{nS}=10 μm, L_{nC}=20 μm and c_0=2 μM

Figure 6 shows that the strong difference of diffusion profile between fluorescent primary proteins alone and fluorescent primary proteins bounded with corresponding proteins complex, is visible over a large range of actuation pressures (from 0.1 to 0.6 bar). We extracted the ratio values D_1/D_2=2±0.2 from best fits along this range of pressures.

The principle of detecting complexing species by differential diffusion rates as described in this paper can be applied to any size of biomolecules by adapting the system as follows: (1) the ratio of the complex diameter to nanoslit height should be as high as possible in order to decrease the effective diffusion and to get a sufficient dispersion area, but it should not be too large to avoid clogging of the nanochannel. (2) There should be sufficient liquid flow in the exit microchannel so that it acts as a sink, provided that it is not high enough to disrupt the semi-circular dispersion profile observed in the nanoslit. This can be assured by maintaining a low ratio between the height of the nanoslit and the microchannel. (3) The driving flow velocity in the nanochannel should be high enough so that the concentration into the nanochannel remains constant, restricting the diffusion gradient to the nanoslit area so that the models in this work remain valid. If a nanochannel system is designed effectively, the limiting factor on sensitivity (low-concentration measurements) will be the detection apparatus.

Conclusions

We have demonstrated a complexing affinity biosensor based on steady-state diffusion effects in nanochannels. We calculated concentration profile over flow velocity, diffusion coefficient, and position as well as measured fluorescence intensity by using a simple flat front model, giving opportunities to predict changes of size of biomolecules in the nanochannel.

We injected fluorescent streptavidin proteins and measured the concentration profile for different nanochannel flow velocities. We added specific biotinylated dextran proteins and measured an important increase of the diffusion length, which was not observed when injecting non-specific wheat germ agglutinin proteins.

Our nanofluidic device provides an interesting solution for simple and rapid detection of protein interactions.

Acknowledgments This work was partially supported by Swiss National Foundation (FNS) grant no. 200021-111790. Cleanroom processing was performed at the EPFL Center of MicroNanoTechnology (CMI). The authors wish to thank Arnaud Bertsch and Kristopher Pataky for reviewing the manuscript.

References

1. Schoch RB (2008) Rev Mod Phys 80:839–883
2. Tegenfeldt JO, Prinz C, Cao H, Huang RL, Austin RH, Chou SY, Cox EC, Sturm JC (2004) Anal Bioanal Chem 378:1678–1692
3. Wang Y-C, Choi MH, Han J (2004) Anal Chem 76:4426–4431
4. Wang Y-C, Stevens AL, Han J (2005) Anal Chem 77:4293–4299
5. Lyon WA, Nie S (1997) Anal Chem 69:3400–3405
6. Williams PS, Levin S, Lenczycki T, Giddings JC (1992) Ind Eng Chem Res 31:2172–2181
7. Hatch A, Kamholz AE, Hawkins KR, Munson MS, Schilling EA, Weigl BH, Yager P (2001) Nat Biotechnol 19:461–465
8. Durand NFY, Bertsch A, Todorova M, Renaud P (2007) Appl Phys Lett 91:203106
9. Panton RL (2005) Incompressible flow. Wiley, New York
10. Cussler EL (1997) Diffusion, mass transfer in fluid systems. Cambridge University Press, UK